

DOUBLE ELECTRON EJECTION IN THE DECAY OF ^{113m}In

K. ILAKOVAC

*Faculty of Science and Mathematics, University of Zagreb, P. O. B. 162, Zagreb
Croatia, Yugoslavia*

Z. KREČAK

Ruder Bošković Institute, P. O. B. 1016, Zagreb, Croatia, Yugoslavia

and

XH. IBRAHIMI

Pedag. Academy, Skopje, Macedonia, Yugoslavia

Received 3 September 1981

UDC 539.16

Original scientific paper

Measurements of double ejection of electrons in the decay of the isomeric state at 391.7 keV in ^{113}In were made. Energy spectra of electrons in KK and $K(L + M + \dots)$ decay were obtained at a relative angle of emission of 60° . The results are compared to various theories. In the energy range accepted, 36—148 keV, the results indicate the predominance of the shake-off process in internal conversion (SOIC) and of the internal conversion in internal Compton effect (ICICE).

1. Introduction

Double electron ejection in the decay of nuclear excited states is one of several possible modes of deexcitation via higher order processes. Due to the interaction of the excited nucleus with the atomic electrons and due to the mutual interactions of electrons, two electrons are emitted from the atom undergoing the nuclear transition. In the process, two holes are created in the atomic shells, and a series

of atomic transitions follows, yielding coincident X rays or Auger electrons and other radiation.

The double electron ejection process may proceed via several mechanisms.

a) Double internal conversion (DIC) proceeds via an intermediate nuclear virtual state: a conversion electron is emitted in a transition to a nuclear virtual state, and by a second electron conversion the nucleus reaches the final state. The process was first considered by Sachs¹⁾, but detailed theoretical considerations were made by Eichler²⁾ and Grechukhin³⁾.

b) Internal conversion of the internal Compton effect (ICICE) is visualized as $E1$ electron conversion process in the internal Compton process. The internal Compton effect (ICE) is a well established process both theoretically^{4,5)} and experimentally⁶⁾. Listengarten⁷⁾ pointed out that the electron conversion of the ICE photon, that is predominantly an $E1$ type transition, should yield double electron ejection. The calculated values of the differential probabilities of ICICE are almost an order of magnitude larger than the experimental values.

c) Shake-off in the internal conversion (SOIC) is a process closely related to the shake-off in beta decay. The latter process was originally studied by Feinberg⁸⁾ and by Migdal⁹⁾. The sudden change of the average Coulomb potential caused by the emission of a particle leads to a finite probability of one (or possibly more) electrons leaving the atom. First estimates of SOIC have been made by Seykora and Waltner¹⁰⁾, and detailed theory was developed by Mukoyama and Shimizu^{11,12)}.

d) The direct collision process (DC) is considered as an internal collision of the outgoing charged particle e. g. beta ray with an electron in the atomic shells via the Coulomb interaction. Feinberg^{8,13)} made estimates of the relative probability of the direct collision and the shake-off processes and found that it is of the order B/E , where B is the binding energy of the outgoing electron and E the energy of the beta particle. On this basis the DC process is generally considered to be negligible.

The review paper of Freedman¹⁴⁾ discusses various effects of atomic shell electrons in nuclear transitions, including the double electron ejection.

Experimental studies of double electron ejection are rather difficult because of the very low probabilities. A previous attempt to observe double electron ejection in the decay of ^{113}In was made by Sommer, Knauf and Klewe-Nebenius¹⁵⁾. They obtained an upper limit $KK/K < 2 \cdot 10^{-5}$ for electrons in the energy range 67 to 268 keV.

In the present investigation ejection of KK and $K(L + M + \dots)$ electron pairs in the decay of the isomeric state of ^{113}In at 391.6 keV was studied. Sharing of energy between electrons in a pair is continuous, but the sum of their energies is subject to energy conservation,

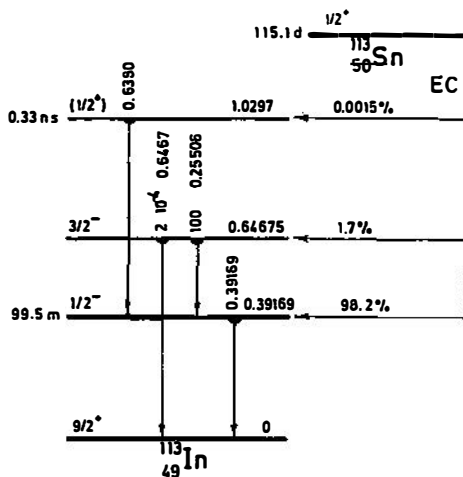
$$E_1 + E_2 = E_0 - B_K - B'_K \quad \text{for } KK \text{ ejection}$$

$$E_1 + E_2 = E_0 - B_K - B'_L \quad \text{for } KL \text{ ejection, etc.,}$$

where E_0 is the transition (gamma-ray) energy, B_K the binding energy of a K shell electron in the atom, and B'_K, B'_L , etc. are the binding energies of a $K-$, $L-$, etc. shell electron in the atom with one hole in the K shell. The above conditions of constant sum-energy and the condition of simultaneity were used in the identification of data.

2. Apparatus and measurements

The source was prepared from a fresh shipment of $^{113\text{m}}\text{Sn}$, supplied by the New England Nuclear Co., U. S. A. The backing was a Zapon foil about $80 \mu\text{g}/\text{cm}^2$ thick, mounted over a 30 mm diam. hole in a lightweight plexiglass holder. To reduce static charges a $20 \mu\text{g}/\text{cm}^2$ thick aluminium film was evaporated on one side of the foil. On the other side a small droplet of $^{113}\text{Sn Cl}_2$ in a 0.1 M HCl solution was placed and slowly dried. Diameter of the source was about 5 mm. Initial strength of the source was $(6.3 \pm 0.30) \mu\text{Ci}$, as determined by means of a Ge (Li) detector and a set of calibrated sources. The decay scheme of ^{113}Sn is shown in Fig. 1.

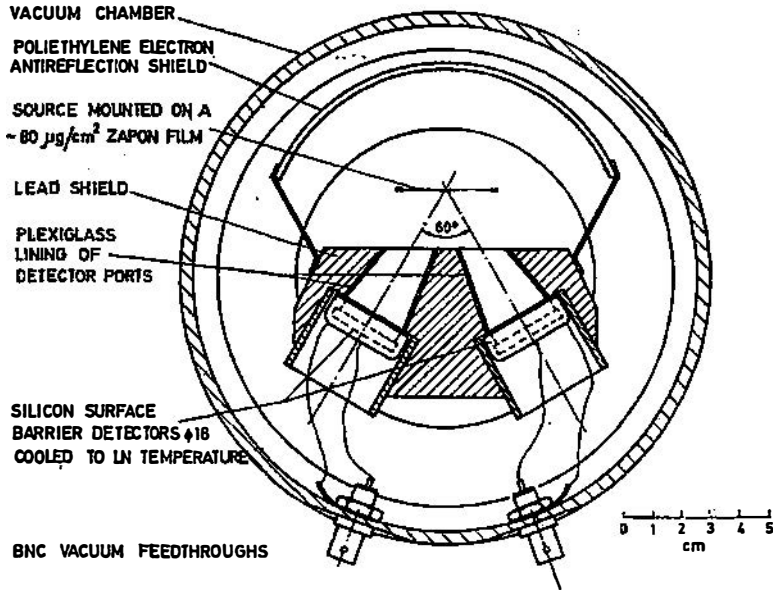


1. Decay scheme of $^{113\text{m}}\text{Sn}^{16}$. The 99.5 min isomeric state decays 64% by gamma emission, 36% by electron conversion ($K/L_1/L_2/L_3/M/N = 100/13.5/2.0/2.65/4.22/0.88$), and with a very small probability by double decay.

The source, lead shield with electron detectors, and electron antireflection shield were mounted on an aluminium plate fixed on top of a copper dipstick inside a vacuum chamber (see Fig. 2). Great care was taken to reduce the scattering of conversion electrons from one detector into the other. The conical openings in the lead shield and the front side of the lead shield were lined with plexiglass. The electron antireflection shield was made of polyethylene and was placed at such a distance that the same parts of the shield were not viewed by both electron detectors.

The electron detectors were made in our laboratory from two discs of monocrystalline silicon, 28 mm diam. \times 2.5 mm thick (donated by Soc. des Mines et Fonderies de Zinc de la Vieilles-Montagne, Belgium). The diameter of the sensitive area was 18 mm, the thickness of the depleted region about 0.8 mm (bias voltage was 800 V), and the thickness of the golden front contact was about $40 \mu\text{g}/\text{cm}^2$. The discs were loosely mounted in teflon housings to allow cooling to liquid air temperature (via the copper dipstick). The contacts were made with thin golden wires and silver paint. The angle between centerlines from the source to the detectors

was close to 60° , and each detector had an angular halfwidth of 9° . Therefore, the extreme angles of relative emission of electrons accepted by the detectors were 42° and 78° .

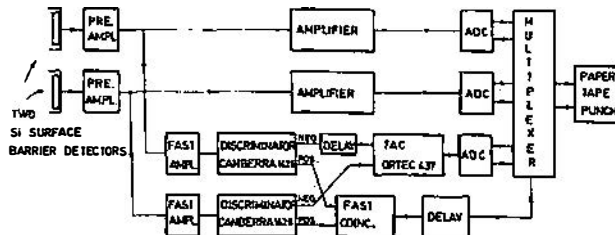


2. A view from above the apparatus showing the vacuum chamber, ^{113}Sn source, detectors and shields.

The pulses from the detectors were fed via charge sensitive preamplifiers into a fast-slow coincidence system with a three-parameter pulse-height analyzer¹⁶⁾ (See Fig. 3). For each coincidence amplitudes of pulses from both detectors, and the time difference, were recorded on punched paper tape. The energy resolution of the detectors (cooled to liquid air temperature) was 6.1 keV and 8.3 keV, respectively, and the time resolution was about 35 ns.

The data were collected for 32 days, with a total running time of 722 hours. In that time from the source a total number of $N_R = (14.6 \pm 0.7) \cdot 10^{10}$ K conversion electrons was emitted. The total number of coincidences was about 560 000.

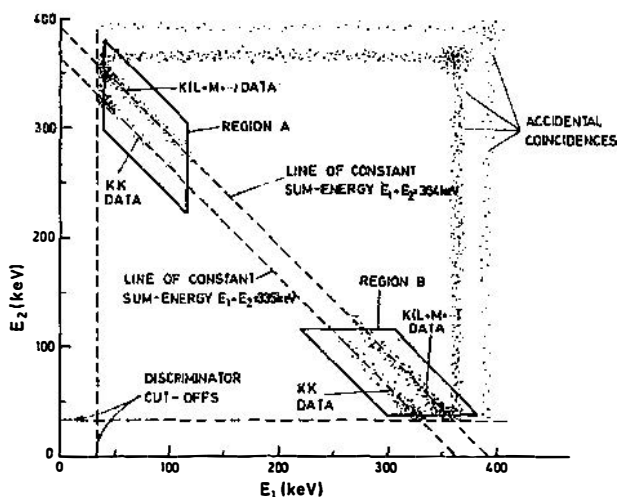
The paper-tape records were transcribed onto magnetic tape and subsequently various output tables were prepared for the analysis.



3. Block diagram of the electronic apparatus.

3. Analysis of data and results

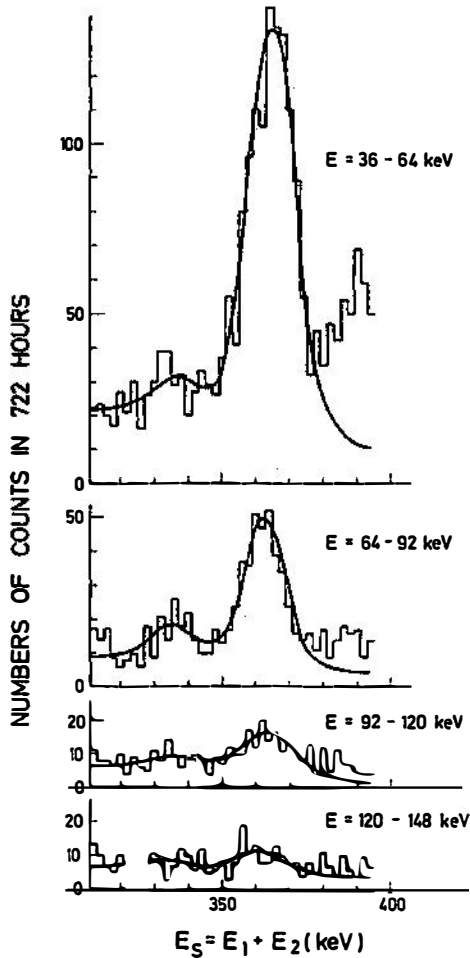
The singles spectra (self-gated and direct) were used to determine the discriminator efficiencies and cut-offs. Energy scale (channel number to electron energy calibration) for either detector was determined from the projections of the coincidence events on the energy axes. Location of the data in the time dimension was determined from the projections of the $E_1 - E_2$ regions corresponding to either KK or $K(L + M + \dots)$ events onto the time axis. The time channels, accepted for the preparation of $E_1 - E_2$ two-parameter tables, were selected from these »time« diagrams, and on this basis the coincidence efficiency, ε_c , was calculated. Since the data were mainly concentrated in the regions of low E_1 (high E_2) and low E_2 (high E_1), each of these regions (region *A* and region *B* in Fig. 4) was separately



4. Schematic diagram of the data in the $E_1 - E_2$ plane. In the final analysis data in the regions *A* and *B* were overlapped.

analyzed. For the final analysis the regions *A* and *B* were overlapped (low E_1 and low E_2 data). In this way tables of numbers of events as a function of $E = E_1 = E_2$, the energy of the »lower energy electron«, and of $E_1 + E_2$, the sum energy, were obtained. For the analysis of KK events, because of low statistics, the E channels were grouped by 14, obtaining four energy regions $\Delta E = 28$ keV wide. The results are shown in Fig. 5. The same data were grouped by 4 channels ($\Delta E = 8$ keV) for the analysis of $K(L + M + \dots)$ events (Fig. 6). In these diagrams a distinct peak at the energy about 362 keV is ascribed to the $K(L + M + \dots)$ process, and the small peak at the energy 335 keV to the KK events.

To determine the numbers of counts due to the KK and $K(L + M + \dots)$ decay the sum-energy spectra shown in Figs. 5 and 6 were analyzed by a curve-fit-

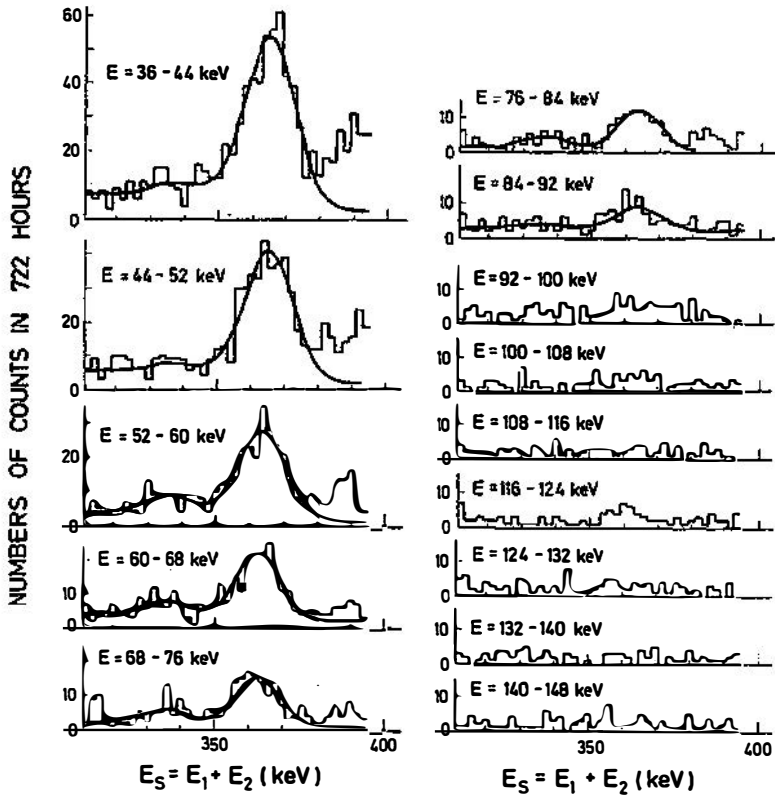


5. Sum energy spectra for 28 keV intervals of energy of the «lower-energy» electron. Full curves were calculated by a minimum chi square fitting procedure.

ting procedure based on minimum chi square. The fitting function of the argument $E_s = E_1 + E_2$, the sum energy, was

$$\begin{aligned}
 f(E_s) = & a_2 \left[\exp \left(-\frac{(E_s - a_3)^2}{2a_6^2} \right) + a_7 \frac{1}{\exp \left(\frac{E_s - a_3}{a_8} \right) + 1} \right] + \\
 & + a_3 \left[\exp \left(-\frac{(E_s - a'_3)^2}{2a_6'^2} \right) + a_7 \frac{1}{\exp \left(\frac{E_s - a'_3}{a_8} \right) + 1} \right] + a_4. \quad (1)
 \end{aligned}$$

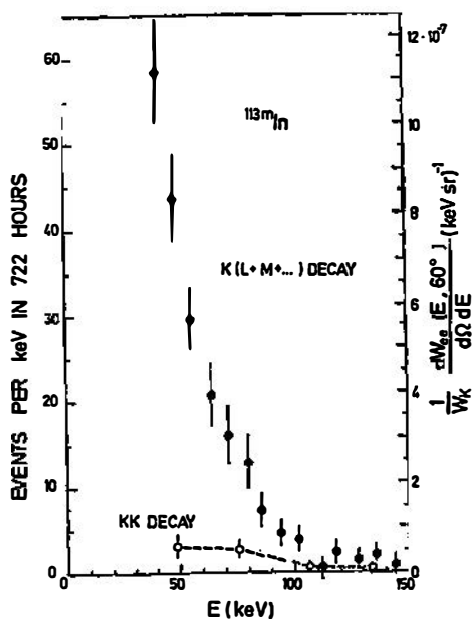
The first bracket represents the $K(L + M + \dots)$ peak at the position a_5 , and the second bracket the KK peak at the position a'_5 . In all calculations $a_5 - a'_5$ was kept constant, 28 keV, the expected difference in position of the two peaks. The parameter a_7 was derived from the singles spectra and was kept at a value of 0.08. The spectra with better statistics were analyzed by varying other parameters. Based on results of these calculations the values of parameters a_5 , a_6 and a_8 were fixed in the analyses of the remaining spectra.



6. Sum energy spectra for 8 keV intervals of energy of the 'lower-energy' electron. Full curves were calculated by a minimum chi square fitting procedure.

An alternative method of analysis, based on five regions of E_s (a region at the KK peak, a region at the $K(L + M + \dots)$ peak, and regions left, between and right of the first two regions) and a curve calculated by a folding procedure of singles' peak of K conversion electrons from the two detectors, was also applied. The results of the two analyses are in a reasonable agreement.

The results of the curve-fitting calculations are shown in Figs. 5 and 6 as full curves. From these fits the numbers of counts Δn_{ee} , shown in Table 1 and Table 2, and in Fig. 7, were calculated.



7. Numbers of events and differential probabilities for the KK and $K(L+M+...)$ decay of the 392 keV state in ^{113m}In .

Table 1.

Electron energy E (keV)	Number of counts Δn_{KK}	$\frac{1}{W_K} \frac{dW_{KK}(E, 60^\circ)}{d\Omega}$ (keV sr) $^{-1}$	$\frac{1}{W_K} \frac{dW_{KK}(E)}{dE}$ (keV) $^{-1}$
36 – 64	84 ± 37	$(5.7 \pm 2.6) \cdot 10^{-8}$	$(7.2 \pm 3.3) \cdot 10^{-7}$
64 – 92	73 ± 27	$(5.0 \pm 1.9) \cdot 10^{-8}$	$(6.3 \pm 2.4) \cdot 10^{-7}$
92 – 120	17 ± 17	$(1.2 \pm 1.2) \cdot 10^{-8}$	$(1.5 \pm 1.5) \cdot 10^{-7}$
120 – 148	13 ± 16	$(0.9 \pm 1.1) \cdot 10^{-8}$	$(1.1 \pm 1.4) \cdot 10^{-7}$
Total 36 to 148 keV	187 ± 51	$(3.6 \pm 1.0) \cdot 10^{-6} \text{ (sr)}^{-1}$	$(4.5 \pm 1.3) \cdot 10^{-5}$

Numbers of counts due to KK decay of ^{113m}In per 28 keV energy intervals of the lower energy electron, obtained at 60° , and the derived differential probabilities (the values in column 4 were obtained from the values in column 3 by multiplying by 4π , based on the assumption of anisotropic angular distribution).

Table 2

Electron energy E (keV)	Number of counts $n_{K(L+...)}$	$\frac{1}{W_K} \frac{dW_{K(L+M+...)}(E, 60^\circ)}{d\Omega dE}$ $10^{-7} (\text{keV sr})^{-1}$	$\frac{1}{W_K} \frac{dW_{A(L+M+...)}(E)}{dE}$ $10^{-6} (\text{keV})^{-1}$
36 - 44	468 ± 49	11.2 ± 1.4	14.1 ± 1.8
44 - 52	349 ± 40	6.7 ± 0.9	8.4 ± 1.1
52 - 60	235 ± 29	5.6 ± 0.8	7.1 ± 1.0
60 - 68	166 ± 30	4.0 ± 0.8	5.0 ± 1.0
68 - 76	129 ± 27	3.1 ± 0.7	3.9 ± 0.9
76 - 84	103 ± 25	2.5 ± 0.6	3.1 ± 0.8
84 - 92	58 ± 16	1.4 ± 0.4	1.7 ± 0.5
92 - 100	37 ± 13	0.9 ± 0.3	1.1 ± 0.4
100 - 108	32 ± 11	0.8 ± 0.3	1.0 ± 0.4
108 - 116	5 ± 10	0.1 ± 0.2	0.15 ± 0.3
116 - 124	19 ± 11	0.5 ± 0.3	0.6 ± 0.3
124 - 132	13 ± 10	0.3 ± 0.2	0.4 ± 0.3
132 - 140	18 ± 8	0.4 ± 0.2	0.5 ± 0.2
140 - 148	7 ± 9	0.2 ± 0.2	0.2 ± 0.3
Total 36 to 148 keV	1639 ± 90	$(3.14 \pm 0.28) \cdot 10^{-5} (\text{sr})^{-1}$	$(3.95 \pm 0.36) \cdot 10^{-4}$

Numbers of counts due to $K(L + M + \dots)$ decay of $^{113\text{m}}\text{In}$ per 28 keV energy interval of the *slower energy* electron, obtained at 60° , and the derived differential probabilities.

External scattering of $^{113\text{m}}\text{In}$ K conversion electrons on K electrons of tin or indium atoms in the source yielded coincident events that were indistinguishable from the true KK double ejection in the above described apparatus. The yield of external scattering was estimated using the Mott formula for electron-electron scattering, that was transformed to obtain $d\sigma_{\text{Mott}}/dE$. Further, from the specification of the shipment of ^{113}Sn from which the source was made (1.0 mg of dry Sn Cl_2 per ml, and 8 mCi of ^{113}Sn per ml of the solution) it was estimated that about 0.5 μg of Sn (and In) was contained in the source used in the measurements. When a uniform thickness of Sn Cl_2 layer was assumed, one obtained a surface density of $1.3 \cdot 10^{16}$ atoms/ cm^2 . The calculated values of probability of external collision per keV and per emitted K conversion electron were obtained by multiplying $d\sigma_{\text{Mott}}/dE$ by the surface density of K electrons of Sn ($2.6 \cdot 10^{16} \text{ cm}^{-2}$).

The values of $\frac{1}{W_K} \frac{dW_{KK}^{\text{ext}}}{dE}$ obtained in this way were 1—2% of the experimental values shown in Table 1. Nonuniformity of the source would increase these percentages by a factor approximately equal to the reciprocal value of the coverage factor. A visual inspection of the source under a microscope revealed some nonuniformity. A rather conservative estimate of the coverage of 0.2 would yield a 5—10% contribution of external scattering. These values should be reduced by a factor of about 2 to take into account the average electron path-length in the source. A fur-

her factor of about 5 should be applied to take into account that elastically scattered electrons peak at a relative angle of 80° to 90°, while the detectors were accepting coincident electrons at a maximum angle of 78° (medium angle was 60°).

Based on these considerations it was estimated that external scattering yielded less than 3% to the observed numbers of events, and it was neglected in the analysis of *KK* decay.

Similar considerations of the contribution of external scattering to the observed numbers of events in *K(L + M + ...)* decay yielded values about 5 times larger. Since realistic estimates were rather difficult, numbers of counts were not corrected for the contribution of external scattering. It should be noted, however, that the stated values may be up to 15% higher than the real values of *K(L + M + ...)* decay.

The differential probability of double electron ejection per *K* electron was calculated from the formula

$$\frac{1}{W_K} \frac{dW_{ee}(E, 60^\circ)}{dE d\Omega} = \frac{1}{2} \frac{4\pi \Delta n_{ee}(E, \Delta E, 60^\circ)}{N_K \Omega_1 \varepsilon_1(E) \Omega_2 \varepsilon_2(E') \varepsilon_c \Delta E} \quad (2)$$

The factor $\frac{1}{2}$ enters because the low E_1 and low E_2 data were overlapped. The solid angles of the detectors were calculated from the geometry of the arrangement, $\Omega_1 = \Omega_2 = 8.71 \cdot 10^{-2}$. The relative full-energy peak efficiencies for *K* conversion electrons of ^{113m}In were determined from the measured activity of the source and the singles' counting rates. The same energy range of 31 keV about the peaks was taken as in the determination of Δn_{ee} from the fits. The values $\varepsilon_1(364 \text{ keV}) = 0.516$ and $\varepsilon_2(364 \text{ keV}) = 0.606$ were obtained. Based on measurements of Jardine and Lederer¹⁷⁾ it was assumed that the relative efficiency of either detector used in the measurements of double electron ejection was independent of electron energy, i. e. that $\varepsilon_1(E = 36 \text{ to } 148 \text{ keV}) = 0.516$ and $\varepsilon_2(E = 36 \text{ to } 148 \text{ keV}) = 0.606$. The efficiency of the coincidence was $\varepsilon_c = 0.95 \pm 0.05$.

The results of the calculations are shown in Table 1 and Table 2 and in Fig. 7.

From the integral numbers of counts the differential probabilities of *KK* and *K(L + M + ...)* decay in the energy range 36 keV to 148 keV of the «lower energy electron» were determined

$$\frac{1}{W_K} \frac{dW_{KK}(E = 36 \text{ to } 148 \text{ KeV}, 60^\circ)}{d\Omega} = (3.6 \pm 1.0) 10^{-6} (\text{sr})^{-1} \quad (3)$$

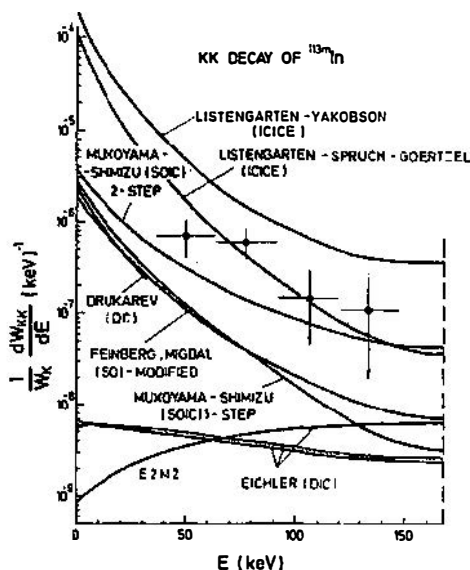
and

$$\frac{1}{W_K} \frac{dW_{K(L+M+\dots)}(E = 36 \text{ to } 148 \text{ keV}, 60^\circ)}{d\Omega} = (3.14 \pm 0.28) 10^{-5} (\text{sr})^{-1}. \quad (4)$$

All quoted errors are standard errors. As discussed above, the *K(L + M + ...)* value may be up to 15% too large, because the possible contribution of external scattering was not subtracted.

4. Discussion

The theories of double electron ejection described in the *Introduction* do not give angular distributions of the electron pairs. Therefore, a direct comparison of the above reported experimental data, obtained at a relative angle of emission of 60° , could not be made. To make a comparison possible, an isotropic angular distribution was assumed: the values of the differential probabilities (third columns in Tables 1 and 2) were multiplied by 4π to obtain energy distributions (fourth columns). These *extrapolated* values are compared to the values derived from the theories of double electron ejection in Fig. 8. for KK decay and in Fig. 9 for $K(L + M + \dots)$ decay.

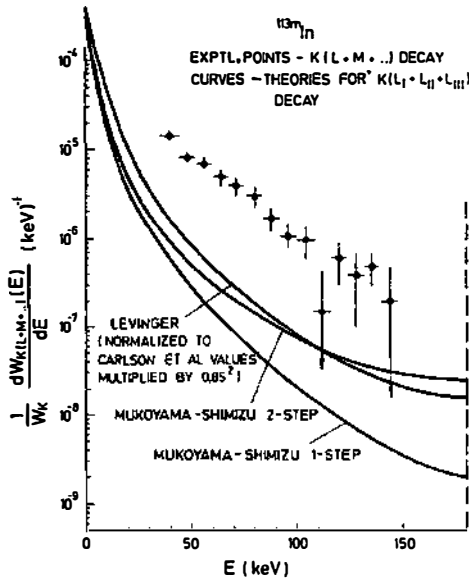


8. Comparison of the experimental energy distribution of KK decay of ^{113m}In (derived on the assumption of an isotropic angular distribution) and of the theoretical energy distributions (full curves) based on theories of Eichler²⁾, of Feinberg³⁾, and of Migdal⁹⁾, multiplied by $(5/16)$ following the estimate of Seykora and Waltner¹⁰⁾, of Drukarev²¹⁾, of Listengarten⁷⁾, and of Mukoyama and Shimizu for the 2-step¹¹⁾ and 1-step¹²⁾ model of KK decay.

The DIC process is very unlikely to be observed in KK decay of ^{113m}In . The curves shown in Fig. 8, calculated from the theory of Eichler²⁾ assuming a relative probability of $\gamma\gamma/\gamma = 10^{-5}$, $\gamma\gamma$ energy distributions as given by Grechukhin³⁾, and electron conversion coefficients of Sliv and Band²⁰⁾, are about three orders of magnitude smaller than the experimental values. Only lowest contributions of multipoles were considered ($E2 M2$, $E3 M1$, and $E1 M3$), since other contributions have still smaller probabilities.

Drukarev²¹⁾ made calculations that according to the Feynman diagram in his paper represent the DC process. The curve in Fig. 8, describing his results, was obtained by reading of values from a diagram and by normalization to the total probabilities KK/K as given in his paper.

The values for the ICICE process were calculated from the estimates of Listengarten⁷⁾, based on ICE coefficients of Jakobson²²⁾, and using the $E1$ electron conversion coefficients of Sliv and Band²⁰⁾ (the *Listengarten-Yakobson* curve in Fig. 8). The values are about 4 times larger than the experimental values. The ICE coefficients of Jakobson are rough estimates of ICE probabilities. The measurements⁶⁾ support the theory of Spruch and Goertzel⁴⁾. When the over-angle-integrated ICE coefficients of Spruch and Goertzel and the internal conversion coefficients of Hager and Seltzer²⁶⁾ were used, one obtained the values shown in Fig. 8 by the curve *Listengarten-Spruch-Goertzel*, that are in a reasonable agreement with the experimental data.



9. Comparison of the experimental energy distribution of $K(L + M + \dots)$ decay of ^{113m}In (derived on the assumption of an isotropic angular distribution) and of the theoretical energy distributions (full curves) based on the theories of Levinger²³⁾ (normalized to the integral probabilities of Carlson et al²⁵⁾ that were multiplied by the factor 0.85^2), and of Mukoyama and Shimizu for the 2-step¹¹⁾ and 1-step¹²⁾ mechanism. It should be noted that the theoretical distributions do not include KM and KN decay.

The SO energy distribution of Feinberg⁸⁾ and Migdal⁹⁾ was modified to take into account a smaller effective change of the central potential when a K electron is emitted as compared to β^- decay. The value $\Delta z = 5/16$, suggested by Seykora and Waltner¹⁰⁾, was taken. This reduced all values of SO probabilities by a factor close to 10.

Mukoyama and Shimizu have developed rather elaborated theories of SOIC considering it as a two-step process¹¹⁾ (electron conversion and SO) and as a one-step process¹²⁾. The results of their calculations based on one-step theory are close to the results of the modified Feinberg and Migdal theory. The two-step model yielded considerably larger values. The one-step model is considered as more realistic.

From the comparison of results of our measurements to the calculated energy distributions one can conclude that in the energy range 36 to 148 keV major contributions to the KK decay are due to the ICICE and SOIC processes. The ICICE process (*Listengarten-Spruch-Goertzel*), when integrated over the whole energy range, yields a total relative probability $KK/K = 10.5 \cdot 10^{-4}$. This value is too large by about an order of magnitude. However, most of the contribution to the integral is due to the low energy region. Integrated probability above 36 keV amounts to $6.9 \cdot 10^{-5}$. One can conclude that the ICICE process does not contribute to the KK decay below about 50 keV as predicted by the simple theory of Listengarten.

The value of the differential probability for the energy interval 36 to 148 keV, Eq. (3), when extrapolated assuming an isotropic angular distribution, yields

$$\frac{1}{\overline{W}_K} W_{KK} (36 \text{ to } 148 \text{ keV}) = (4.5 \pm 1.3) \cdot 10^{-5}.$$

For the calculation of the total relative probability of KK process an extrapolation of the energy distribution below 36 keV is required. The extrapolation is rather uncertain, because various theoretical energy distributions give different fractions of the total relative probability for the energy range 36 to 148 keV, and because of the uncertainty of the shape of these distributions. E. g. if the energy distribution of the Mukoyama-Shimizu two-step model is assumed, the energy interval 36—148 keV encompasses about 22% of the total probability. With this assumption, and the assumption of an isotropic angular distribution, one obtains

$$\frac{1}{\overline{W}_K} W_{KK} = (2.0 \pm 0.6) \cdot 10^{-4}.$$

The results for $K(L + M + \dots)$ decay are compared to the theoretical energy distributions for KL decay in Fig. 9. The energy distribution shown by the upper curve was calculated from the Levinger's^{2,3)} formulas for KL_1 , KL_2 , KL_3 shake-off probabilities in β^- decay. The normalization was made using the results of Carlson et al^{2,4)} for the total relative probabilities of L shake off in β^- decay, and by multiplying these values by the factor 0.852^2 to take into account the reduced change of the average Coulomb potential in K conversion^{2,5)}.

The differential probabilities of the Mukoyama and Shimizu theories for the two-step and one-step mechanism in KL decay are shown by the other two curves.

The results of our measurements for the $K(L + M + \dots)$ decay are more than an order of magnitude larger than the theoretical results. Corrections for external scattering in the source were estimated to require a reduction of experimental values by up to 15%. KM and KN processes have not been included in the theoretical distributions because of the lack of data. Other processes may also be of importance in the energy region 36 to 148 keV.

When an isotropic angular distributions is assumed one obtains the relative probability of $K(L + M + \dots)$ decay

$$\frac{1}{\overline{W}_K} W_K(L + M + \dots) (36 \text{ to } 148 \text{ keV}) = (4.2 \pm 0.4) \cdot 10^{-4}.$$

Acknowledgments

The authors express their warm thanks to Dr. T. Mukoyama for sending the results of calculations of SOIC for ^{113m}In . Many thanks are due to the late Dr. M. Konrad of the Electronics Dept., Institute R. *Bošković* for the help with the electronic apparatus, to Mrs. N. Ilakovac for the preparation of the electron detectors, and to Mr. J. R. Cushing for the reading of the manuscript.

References

- 1) R. G. Sachs, Phys. Rev. **57** (1940) 194;
- 2) J. Eichler, Z. Phys. **160** (1960) 333;
- 3) D. P. Grechukhin, Yad. Fiz. **4** (1966) 497 (transl.: Sov. J. Nucl. Phys. **4** (1967) 354);
- 4) L. Spruch and G. Goertzel, Phys. Rev. **94** (1954) 1671;
- 5) K. Baumann and H. Robl, Z. Naturforsch. **9a** (1954); 511;
- 6) E. Fuschini, C. Maroni, and P. Veronesi, Nuovo Cimento **26** (1962) 831, **41 B** (1966) 252; A. Ljubičić et al, Phys. Rev. **C3** (1971) 824; M. Jurčević et al, Phys. Rev. **C11** (1975) 1312;
- 7) M. A. Listengarten, Vestn. Leningr. Univ., Ser. Fiz. Khim. **16** (1962) 142;
- 8) E. L. Feinberg, J. Phys. (USSR) **4** (1941) 423;
- 9) A. Migdal, J. Phys. (USSR) **4** (1941) 450;
- 10) E. J. Seykora and A. W. Waltner, Am. J. Phys. **38** (1970) 542;
- 11) T. Mukoyama and S. Shimizu, Phys. Rev. **C11** (1975) 1353;
- 12) T. Mukoyama and S. Shimizu, Phys. Rev. **C13** (1976) 377;
- 13) E. L. Feinberg, Yad. Fiz. **1** (1965) 612;
- 14) M. S. Freedman, Ann. Rev. Nucl. Sci. **24** (1974) 209;
- 15) H. Sommer, K. Knauf, and H. Klewe-Nebenius, Z. Physik **216** (1968) 153;
- 16) C. M. Lederer and V. S. Shirley, *Table of Isotopes*, Wiley-Interscience, New York 1978;
- 17) N. Bogunović, F. Jović, M. Konrad, and Ž. Posavec, Proc. V Congress Mat., Phys. and Astr. of Yugoslavia, Skopje 1972;
- 18) L. J. Jardine and C. M. Lederer, Nucl. Instrum. Methods **120** (1974) 515;
- 19) D. P. Grechukhin, Nucl. Phys. **35** (1962) 98;
- 20) L. A. Sliv and I. M. Band, *Coefficients of Internal Conversion of Gamma Radiation*, Acad. Sci. USSR, Moscow-Leningrad 1956, 1958, and 1961. Graphs in ref. 16;
- 21) E. G. Drukarev, Yad. Fiz. **21** (1975) 593;
- 22) A. M. Yakobson, Zh. Eksp. Teor. Fiz. **29** (1955) 703;
- 23) J. S. Levinger, Phys. Rev. **90** (1953) 11;
- 24) T. A. Carlson, C. W. Nestor, Jr., T. C. Tucker, and F. B. Malik, Phys. Rev. **169** (1968) 27;
- 25) F. T. Porter, M. S. Freedman, and F. Wagner, Phys. Rev. **C3** (1971) 2246.

DVOELEKTRONSKI RASPAD ^{113m}In

K. ILAKOVAC

Prirodoslovno-matematički fakultet, Zagreb

Z. KREČAK

Institut »Ruder Bošković«, Zagreb

i

XH. IBRAHIMI

Pedagoška akademija, Skopje

UDK 539.16

Originalni znanstveni rad

Izvršena su mjerenja dvoelektronskog raspada u raspadu izomernog stanja na 391.7 keV u ^{113m}In . Postignuti su energetske spektri elektrona iz KK i $K(L + M + \dots)$ raspada na kutu razleta od 60° . Načinjene su usporedbe s nizom teorija. U području energije 36—148 keV, koje je prihvaćeno u mjerenju, rezultati ukazuju da dominiraju proces otresanja u unutrašnjoj konverziji (SOIC) i unutrašnja konverzija pri unutrašnjem Comptonovom efektu (ICICE).